Intercomparison of Aircraft and Buoy Measurements of Wind and Wind Stress during SMILE*

ROBERT C. BEARDSLEY

Physical Oceanography Department, Woods Hole Oceanographic Institution, Woods Hole, Massachusetts

AMELITO G. ENRIQUEZ AND CARL A. FRIEHE

Engineering Department, University of California, Irvine, Irvine, California

CAROL A. ALESSI

Physical Oceanography Department, Woods Hole Oceanographic Institution, Woods Hole, Massachusetts

8 July 1996 and 24 December 1996

ABSTRACT

An intercomparison between low-level aircraft measurements of wind and wind stress and buoy measurements of wind and estimated wind stress was made using data collected over the northern California shelf in the Shelf Mixed Layer Experiment (SMILE). Twenty-five buoy overflights were made with the NCAR King Air at a nominal altitude of 30 m over NOAA Data Buoy Center (NDBC) environmental buoys 46013 and 46014 between 13 February and 17 March 1989; meteorological conditions during this period were varied, with both up- and downcoast winds and variable stability. The buoy winds measured at 10 m were adjusted to the aircraft altitude using flux profile relations, and the surface fluxes and stability were estimated using both the TOGA COARE and Large and Pond bulk parameterizations.

The agreement between the King Air wind speed and direction measurements and the adjusted NDBC buoy wind speed and direction measurements was good. Average differences (aircraft − buoy) and standard deviations were 0.6 ± 0.8 m s^{-1} for wind speed and $0.0° \pm 10.5°$ for direction (adjusted for buoy offset), independent of parameterization used.

The comparisons of aircraft and buoy wind stress components also showed good agreement, especially at larger values of the wind stress (>0.1 Pa) when the wind stress field appeared to be more spatially organized. For the east component, the average difference and standard deviation were 0.018 ± 0.029 Pa using TOGA COARE and -0.018 ± 0.027 Pa using Large and Pond. For the north component, the average difference and standard deviation are 0.003 ± 0.018 Pa using TOGA COARE and 0.003 ± 0.017 Pa using Large and Pond. These results support the idea that low-flying research aircraft like the King Air can be used to accurately map both the surface wind and the surface wind stress fields during even moderate wind conditions.

1. Introduction

During the Shelf Mixed Layer Experiment (SMILE) conducted over the northern California shelf in winter 1988–89, aircraft measurements of wind and wind stress were made at a nominal altitude of 30 m (100 ft) with the National Center for Atmospheric Research (NCAR) King Air over NOAA Data Buoy Center (NDBC) environmental buoys 46013 (NDBC13) and 46014 (NDBC14) (Fig. 1). These aircraft measurements were made during a sequence of flights that included both low-level horizontal legs designed to map the wind and wind stress fields just above the ocean surface and ascending–descending legs designed to examine the vertical structure of the marine layer during winter conditions (Friehe et al. 1991).

A key hypothesis behind these flights and their interpretation is that the wind stress pattern deduced from the 30-m aircraft measurements accurately reflects the surface wind stress field, that is, that the constant-flux layer in the atmosphere extends up at least 30 m above the ocean surface so that the 30-m and surface stress fields are nearly equal in both spatial structure and magnitude. A previous intercomparison between collocated buoy and 30-m aircraft wind measurements made in the same region during generally stable conditions in April–May 1981 with the NCAR Queen Air showed good

*Woods Hole Oceanographic Institution Contribution Number 9379.

Corresponding author address: Dr. Robert C. Beardsley, Department of Physical Oceanography, Woods Hole Oceanographic Institution, Woods Hole, MA 02543.
E-mail: rbeardsley@whoi.edu

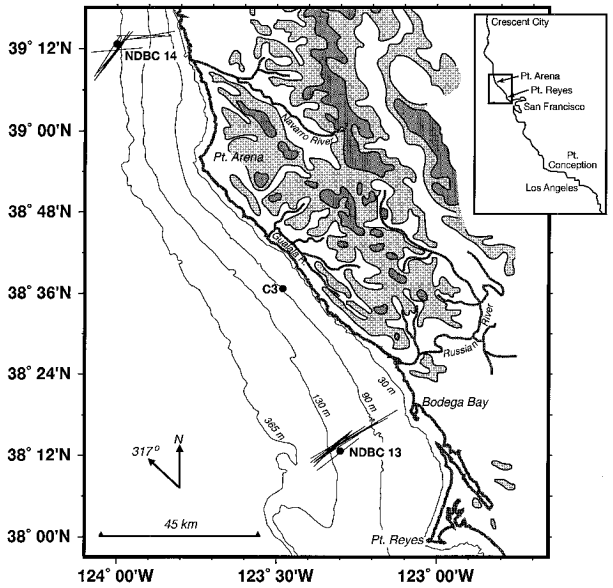

FIG. 1. Map of the northern California shelf showing the locations of NDBC (NOAA Data Buoy Center) environmental buoys 46013 (NDBC13) and 46014 (NDBC14) and the King Air flight tracks made over each buoy. Also shown is the location of the WHOI C3 meteorological buoy where supportive measurements were made. The coastal mountain range is indicated by the 300- and 600-m height contours and shading.

agreement between aircraft wind and adjusted buoy winds; however, a comparison of wind stress was not made at that time (Friehe et al. 1984).

The King Air instrumentation allows direct estimation of wind stress through eddy correlation. This note presents an intercomparison of the King Air wind and wind stress measurements with buoy measurements to help assess how well the 30-m aircraft measurements reflect the surface wind stress field during SMILE.

2. Instrumentation and data processing

The air velocity vector relative to the King Air is measured with a differential pressure sensing system mounted in the nose dome, and the motion of the aircraft relative to the earth is measured with an inertial navigation system with Loran C available for correction. The instantaneous wind velocity components are sampled at 20 Hz with the aircraft flying at a speed of about 70 m s^{-1} at a nominal altitude of 30 m. The mean wind and (eddy correlation) wind stress components are computed using a 180-s averaging period, which corresponds to a spatial average over about 12.6 km. While there are numerous sources of experimental uncertainty in these measurements, conservative estimates of overall accuracy are ± 1 m s^{-1} for wind speed, less than $\pm 15°$ for wind direction for wind speeds greater than 4 m s^{-1}, and ± 0.1 Pa for east and north wind stress components (Miller and Friesen 1985; Enriquez 1994; Enriquez and Friehe 1995).

The NDBC buoys utilize a 10-m discus hull and tower to support an integrated propeller and vane wind and air temperature sensors at a height of 10 m and a water temperature sensor at a depth of 1 m. An R. M. Young wind monitor is used to measure wind speed and direction, with a fluxgate compass attached to the wind monitor vane; the total system accuracy is the greater of ± 1.0 m s^{-1} or 10% in wind speed and $\pm 10°$ in direction (D. Gilhousen 1994, personal communication). Both air and water temperatures are measured with thermistors with an uncertainty of ± 1.0°C. One buoy also measured relative humidity at 10 m with an uncertainty of ± 5% of reading. The buoy wind speed and direction sensors are sampled at 1 Hz for 8.5 min each hour, and the vector average wind speed and direction are recorded hourly (Gilhousen 1987).

A total of 25 buoy overflights were made between 13 February and 17 March 1989, which satisfied two criteria: the aircraft track must pass within 5 km of the buoy (Fig. 1) and the aircraft altitude must be within 5 m of the nominal 30 m. For this intercomparison, buoy wind speed and direction values were interpolated at the midtimes of the aircraft overflights. The individual aircraft tracks were about 12.6 km long and oriented generally in the cross-shelf direction. The mean and maximum horizontal distance between the midpoint of the aircraft tracks (which corresponds to the midtime of the overflight) and the buoys were 3.8 and 9.3 km, respectively.

The buoy wind measurements were adjusted to aircraft height using the flux profile of Businger et al. (1971),

$$U_{\mathrm{Zac}} = U_{\mathrm{Zb}} + \frac{u_*}{k}\left[\ln\left(\frac{\mathrm{Zac}}{\mathrm{Zb}}\right) + \psi_m\left(\frac{\mathrm{Zac}}{L}\right) - \psi_m\left(\frac{\mathrm{Zb}}{L}\right)\right],$$

where U is the wind speed, Zac and Zb are the aircraft and buoy measurement heights, u_* is the friction velocity, $k = 0.40$ (von Kármán's constant), and L is the Monin–Obukhov length. Both u_* and L were computed from the buoy wind speed, relative humidity, and air and water temperature data using two bulk aerodynamic parameterizations, an early version of the TOGA COARE code described by Fairall et al. (1996), and the Large and Pond (1981) formulation. Where relative humidity data were missing, estimates were obtained from relative humidity measurements made on the WHOI meteorological buoy deployed at C3 (Fig. 1; Alessi et al. 1991). The buoy wind stress direction was assumed to be identical to the buoy wind direction.

The two bulk parameterizations chosen for this intercomparison are both characteristic of open-ocean conditions with drag coefficients typically lower than most near-coast or shallow-water parameterizations (Geernaert 1990). This was done for both historical reasons [e.g., the Large and Pond (1981) parameterization has been widely used in both United States east coast and west coast experiments, from the 1981–82 Coastal

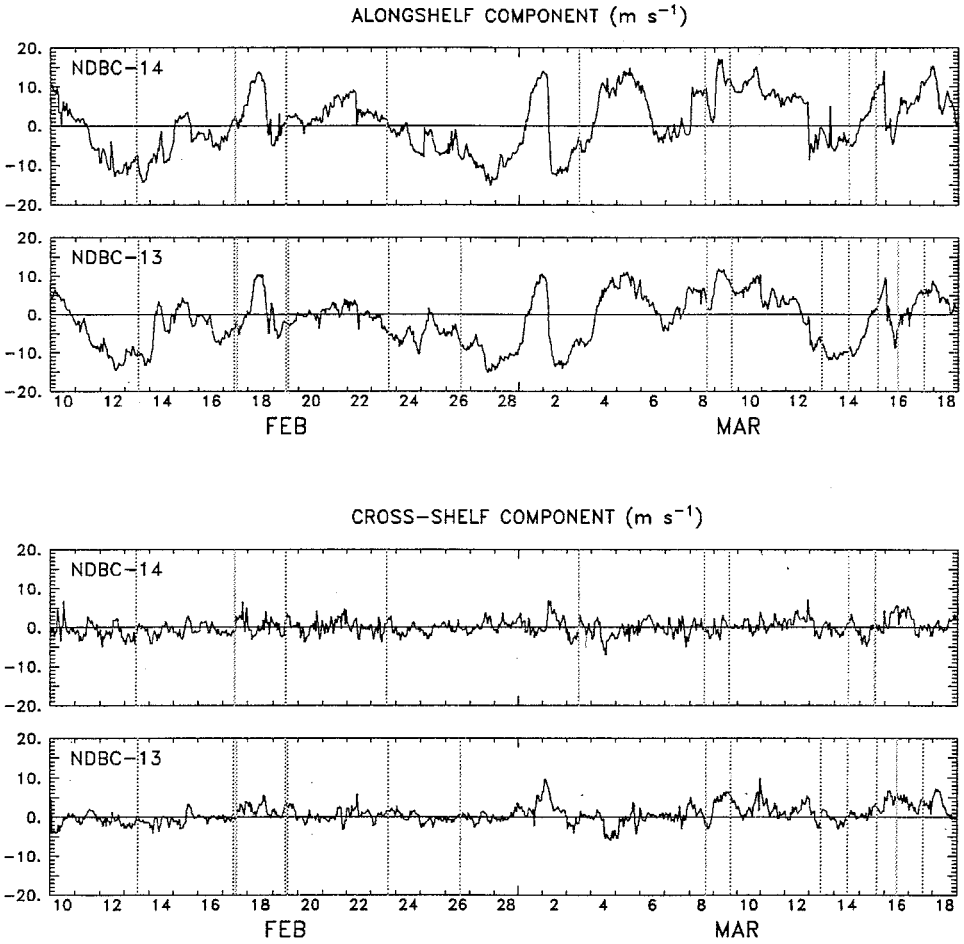

FIG. 2. Along- and cross-shelf 10-m winds measured at NDBC13 and NDBC14. The center times of the buoy overflights considered in this analysis are denoted by vertical lines. Due to the change in the coastline at Point Arena, the positive cross- and along-shelf directions are 72° and 342° for NDBC14 and 32° and 302° for NDBC13 [based on the principal axes analysis given in Table 2 of Dorman et al. (1995)].

Ocean Dynamics Experiment through at least SMILE] and scientific reasons. Enriquez and Friehe (1996) recently found that the parameterization of the drag coefficient using the SMILE aircraft data is in better agreement with previous open ocean parameterizations (e.g., Large and Pond 1981) than with near-coast parameterizations. They attribute this to the direction of the prevailing winds observed over the northern California shelf. In all seasons, the coastal mountain ridge tends to suppress low-level cross-shore winds, resulting in predominantly alongshore winds that tend to produce an along- and onshore wave field that is more characteristic of open-ocean, long-fetch waves superimposed on Pacific Ocean swell (Beardsley et al. 1987; Santala 1991; Dorman et al. 1995). The new TOGA COARE code represents a serious community effort to improve the Liu et al. (1979) bulk formulation for use in the tropical Pacific and elsewhere where unstable conditions can be strong and persistent.

3. Environmental conditions

Dorman et al. (1995) found in their analysis of the surface meteorology during SMILE that the surface wind field was strongly polarized in the along-coast direction due in part to the coastal mountain range (Fig. 1). Time series of along- and cross-shelf wind recorded at NDBC13 and 14 during the period of the King Air measurement program (10 February–18 March) show quite varied conditions, with periods of both strong up- and downcoast winds, with some extended periods of weak winds (Fig. 2). Dorman et al. (1995) developed a simple wind event classification scheme based on NDBC13 wind conditions over a 12-h period, consisting of (a) strong downcoast winds (mean speeds greater than 7.5 m s^{-1}), (b) strong upcoast winds (mean speeds greater than 7.5 m s^{-1}), (c) weak winds (mean speeds less than 4 m s^{-1}), and (d) other. The times of the buoy overflights considered here (also shown in Fig. 2) indicate that the aircraft sampled a variety of conditions,

TABLE 1. Listing of basic buoy and aircraft data used in each buoy overflight comparison considered here. The buoy measurements and derived estimated wind stress magnitude computed using the two parameterizations are given first, followed by the aircraft flight data. The last three columns give the surface Monin–Obukhov length L computed using the TOGA COARE code (with $L > 0$ for stable stratification), the wind event classification (CL) developed by Dorman et al. (1995), and the approximate marine mixed-layer height Z_i during each overflight. The code is N for strong downcoast wind, S for strong upcoast wind, W for weak winds, and indeterminate cases denoted by a dash. The surface mixed-layer heights Z_i are based on vertical soundings made either just before or after a horizontal overflight; if the sounding occurred at a different time (>1 h), the value is marked by an asterisk (Friehe et al. 1991). The case of no apparent mixed layer is noted as <30 m.

				Buoy data						
Flight Buoy No.	Date	Time (PST)	No.	U_b (m s^{-1})	θ_b (°)	RH (%)	T_a (°C)	T_s (°C)	τ_{LP} (Pa)	τ_{TC} (Pa)
14	13 Feb 89	1110:05	4	8.7	357.9	64.1	7.9	10.1	0.116	0.127
13	13 Feb 89	1302:41	4	10.4	311.2	65.0	8.5	9.6	0.164	0.187
13	17 Feb 89	1025:06	6	4.0	306.5	84.0	9.9	9.7	0.024	0.019
14	17 Feb 89	1059:01	6	2.6	130.2	78.9	9.6	10.2	0.011	0.009
13	17 Feb 89	1252:23	6	2.0	303.2	79.3	10.2	10.0	0.007	0.005
13	19 Feb 89	1053:03	7	3.9	255.1	83.4	10.0	10.1	0.023	0.019
14	19 Feb 89	1125:11	7	1.9	171.6	83.6	10.8	10.3	0.006	0.003
14	19 Feb 89	1140:41	7	2.4	216.0	81.8	10.6	10.4	0.009	0.006
13	19 Feb 89	1323:01	7	4.1	254.9	81.4	10.4	10.2	0.025	0.021
14	23 Feb 89	1423:26	9	1.9	186.4	84.3	10.6	11.0	0.006	0.005
13	23 Feb 89	1603:46	9	5.0	292.6	83.5	9.9	10.7	0.038	0.035
13	26 Feb 89	1407:05	10	6.9	306.7	82.7	10.4	10.3	0.068	0.066
14	3 Mar 89	1115:31	13	3.7	361.1	58.8	7.5	10.1	0.024	0.021
14	8 Mar 89	1347:59	16	9.3	152.9	96.5	11.1	10.3	0.121	0.130
13	8 Mar 89	1527:31	16	4.8	118.5	95.3	11.2	10.4	0.031	0.024
14	9 Mar 89	1427:01	17	11.9	157.1	96.5	11.2	10.2	0.216	0.237
13	9 Mar 89	1612:51	17	10.3	168.3	95.2	11.7	10.9	0.151	0.169
13	13 Mar 89	1036:34	19	7.3	325.8	89.3	9.8	11.2	0.081	0.082
13	14 Mar 89	1130:46	20	9.7	309.5	69.5	10.2	11.0	0.139	0.157
14	14 Mar 89	1221:34	20	3.7	323.8	71.5	10.0	10.7	0.022	0.019
14	15 Mar 89	1248:10	21	6.9	161.4	81.8	10.6	10.7	0.069	0.068
14	15 Mar 89	1304:26	21	7.4	159.4	82.2	10.5	10.7	0.081	0.081
13	15 Mar 89	1446:57	21	3.7	199.9	83.2	10.9	11.4	0.021	0.018
13	16 Mar 89	1046:51	22	6.0	262.9	63.8	10.6	11.0	0.054	0.051
13	17 Mar 89	1302:41	23	7.4	167.5	89.1	11.4	11.3	0.078	0.077

with strong up- and downcoast wind conditions representing about 40% of the cases, weak winds another 40%, and the rest classified as other.

Dorman et al. (1995) examined in detail representative examples of strong upcoast (11 February), strong downcoast (8 March), and weak (17 February) wind events. Maps of 30-m wind and wind stress vectors during the strong up- and downcoast examples (their Figs. 11 and 22) exhibit relatively large spatial scales over the shelf north of Point Arena and off Bodega Bay where the buoy overflights examined here were obtained. These results (plus other low-level maps not shown) indicate that the buoy and aircraft measurements (which represent averages over 12.6-km-long tracks) should be directly comparable during periods of moderate to strong winds.

The mean and maximum buoy wind speeds during the buoy overflights were 5.8 and 11.9 m s^{-1}. The mean relative humidity was 81%, and the air–sea temperature difference varied from a minimum of $-2.6°$ to $+1.0°$C, with a mean of 0.3°C. The mean sea surface temperature was 10.5°C. The mean rms wave height and significant wave period were 2.0 m and 7.6 s. While the vertical height of the marine layer typically exceeded 500 m (Dorman et al. 1995), the height of the surface mixed layer Z_i as determined by the vector wind, temperature, and mixing ratio profiles varied from near 0 to 800 m during the overflights considered here. The mean mixed-layer height during the overflights was 256 m. A complete listing of the basic buoy and aircraft measurements plus wind classification and mixed-layer height is given in Table 1.

4. Wind speed and direction comparisons

Using either bulk parameterization, wind speed and direction comparisons show good agreement, with an average difference and standard deviation between aircraft and buoy values of 0.6 ± 0.8 m s^{-1} for wind speed (Table 2; Fig. 3) and $0.0° \pm 10.5°$ for wind direction (Fig. 4). Because of the large potential uncertainty in the wind direction values for each buoy ($\pm 10°$), the mean buoy wind direction was set equal to the mean aircraft wind direction for each buoy in the analysis of the combined data set (Table 2). The largest differences in wind speed and direction are 2.6 m s^{-1} and 29.0°. The correlation coefficients between aircraft and buoy wind speed and direction are 0.97 and 0.99, respectively, independent of choice of bulk parameterization.

TABLE 1. (*Extended*)

Flight data								
U_a (m s^{-1})	θ_a (°)	τ_x (Pa)	τ_y (Pa)	$\lvert\tau\rvert$ (Pa)	θ_τ (°)	L (m)	CL	Z_i (m)
9.1	343.7	−0.072	0.121	0.141	329.3	−79.2	N	680
11.0	312.7	−0.129	0.117	0.174	312.2	−219.3	N	300*
4.9	318.6	−0.048	0.021	0.052	293.3	392.2	W	410
2.8	135.6	−0.011	−0.028	0.030	201.1	−16.8	W	100
2.5	281.8	−0.008	0.002	0.008	285.7	826.4	W	410*
4.9	261.0	−0.012	−0.000	0.012	269.4	−181.8	W	100
2.9	200.6	−0.010	−0.008	0.013	231.6	14.8	W	220
3.7	201.7	0.003	−0.006	0.007	153.0	96.2	W	110
5.2	254.7	−0.024	0.004	0.024	279.9	421.9	W	100*
2.2	198.2	−0.005	0.008	0.009	327.2	−13.7	—	140
6.3	295.3	−0.060	0.036	0.070	300.8	−51.2	—	220
9.7	315.3	−0.097	0.098	0.138	315.3	−1428.6	N	170
3.7	355.1	−0.048	0.043	0.064	312.0	−9.7	—	800
11.8	150.5	0.008	−0.108	0.108	175.7	242.7	S	—
5.8	115.3	−0.019	−0.022	0.029	222.0	44.5	W	38
13.3	155.1	0.076	−0.206	0.220	159.7	377.4	S	<30
12.2	167.8	−0.011	−0.164	0.164	184.0	330.0	S	<30
8.5	321.0	−0.029	0.069	0.075	337.5	−86.6	N	400
11.2	314.2	−0.081	0.096	0.125	319.8	−246.3	N	250
3.9	316.3	−0.018	0.015	0.023	309.7	−28.1	W	600
10.2	169.7	−0.054	−0.083	0.099	212.7	−387.6	S	200
10.5	151.2	0.039	−0.092	0.100	157.3	−355.9	S	100
3.8	187.2	−0.050	−0.045	0.067	227.8	−43.4	W	300
6.9	270.7	−0.045	0.019	0.049	292.6	−96.7	—	400
8.5	164.6	−0.001	−0.081	0.081	180.7	1754.4	—	<30

5. Wind stress comparison

The comparison of aircraft and buoy wind stress magnitude shows reasonable agreement, giving an average difference and standard deviation between aircraft and buoy wind stress magnitudes of 0.010 ± 0.024 Pa using TOGA COARE and 0.012 ± 0.020 Pa using Large and Pond (1981) (Table 2; Fig. 5). The corresponding correlation coefficients are 0.93 and 0.94, respectively.

The aircraft wind direction and wind stress direction differ significantly at lower wind stresses; the average direction difference and standard deviation decreases from 21.5° ± 49.0° below 0.1 Pa to 4.1° ± 17.9° above (Fig. 6). The correlation coefficient between aircraft and buoy wind stress direction is 0.83, with an average difference and standard deviation of 16.8° ± 43.0°.

Several previous field studies have shown systematic differences between the wind and wind stress vector orientations. Geernaert (1988) found a dependence of the angle on atmospheric stability, with the wind stress oriented slightly to the right of the wind for unstable flow and to the left for stable flow. Geernaert et al. (1993) and Rieder et al. (1994) independently found a correlation between the wind stress direction and the direction of the surface gravity waves, with the wind stress vector turning toward the wave propagation direction with decreasing height above the surface. Rieder et al. (1994) found the strongest correlation at high wind speeds during the Surface Wave Processes Program (SWAPP) in the eastern North Pacific, while Geernaert et al. (1993) found the highest correlation at light winds and near-neutral stability conditions during the Surface Wave Dynamics Experiment (SWADE) conducted off Cape Hatteras.

The SMILE data considered here do not exhibit any significant correlation with either stability or wave direction within the limits of the aircraft and buoy experimental uncertainties. In particular, Enriquez and Friehe (1996) found no systematic correlation between stability and the angle between the aircraft wind and wind stress. The large differences in aircraft wind and wind stress directions observed during light winds (with stresses less than 0.1 Pa) can be attributed to two factors: the greater sensitivity of both wind and wind stress direction estimates to experimental uncertainties at lower wind speeds and the higher relative spatial and temporal variability of the winds during lighter winds, making the covariance computations for the stress components less reliable. In addition, the results of Rieder et al.

TABLE 2. Statistical comparison of aircraft and buoy wind and wind stress measurements during SMILE. Statistics are shown for buoys NDBC13 and NDBC14, as well as for the combined buoy dataset. The total number of overflights equals 25. The correlation coefficient is denoted by CC. T/C and L&P designate TOGA COARE and Large and Pond, respectively.

		NDBC13				NDBC14				Combined			
Location:		38°11.98′N, 123°18.00′W				39°11.98′N, 124°00.00′W							
Number of overflights		14				11				25			
		T/C		L&P		T/C		L&P		T/C		L&P	
Variable		Mean	Standard deviation	Mean	Standard deviation	Mean	Standard deviation	Mean	Standard deviation	Mean	Standard deviation	Mean	Standard deviation
Wind speed (m s^{-1})	CC	0.98		0.98		0.97		0.97		0.97		0.97	
		0.49	0.62	0.57	0.59	0.62	1.06	0.74	1.06	0.55	0.83	0.65	0.81
Wind direction (°)	CC	0.99				0.99				0.99			
		8.9	8.8			−7.0	12.9			0.0	10.5		
Wind stress magnitude (Pa)	CC	0.89		0.90		0.97		0.97		0.93		0.94	
		0.010	0.028	0.011	0.024	0.010	0.019	0.012	0.016	0.010	0.024	0.012	0.020
Wind stress direction (°)	CC	0.92				0.74				0.82			
		17.2	28.3			17.4	59.7			17.3	43.8		
τ_x (Pa)	CC	0.84		0.84		0.71		0.69		0.81		0.81	
		−0.010	0.027	−0.013	0.025	−0.026	0.030	−0.024	0.030	−0.018	0.029	−0.018	0.027
τ_y (Pa)	CC	0.96		0.97		0.99		0.99		0.98		0.98	
		0.006	0.020	0.007	0.020	−0.001	0.014	−0.003	0.013	0.003	0.018	0.003	0.017

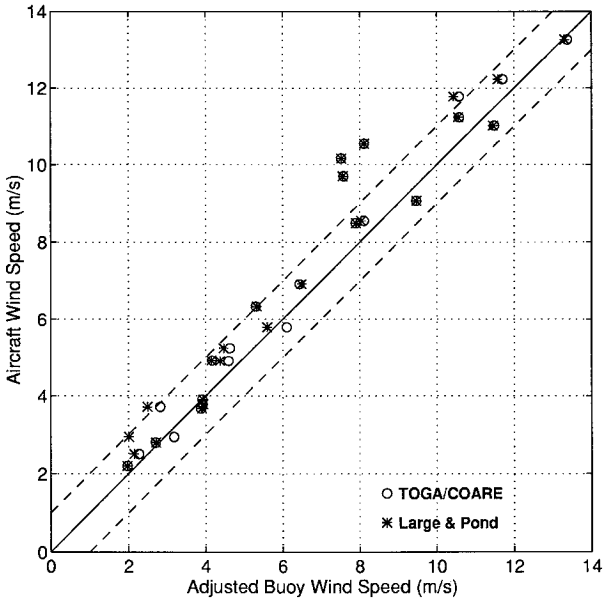

FIG. 3. Comparison of 30-m aircraft wind speed and the 10-m buoy wind speed adjusted to 30 m using the TOGA COARE and Large and Pond (1981) parameterizations. Solid line indicates a one-to-one relationship; dash lines indicate the ±1.0 m s^{-1} difference between aircraft and buoy values. The TOGA COARE and Large and Pond (1981) values are denoted by circles and stars, respectively. See Table 2 for statistical comparisons.

(1994) and Large et al. (1995) suggest that the influence of the surface gravity waves on the wind stress profile and orientation were probably confined to below the buoy and aircraft measurement heights of 10 and 30 m, so that the lack of a significant difference in direction between the aircraft wind and wind stress vectors is perhaps not too surprising. Recent measurements from

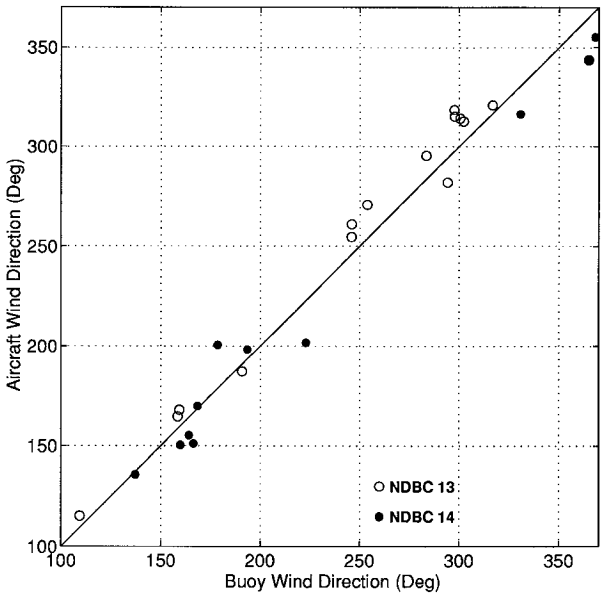

FIG. 4. Comparison of the 30-m aircraft wind direction and the 10-m buoy wind directions.

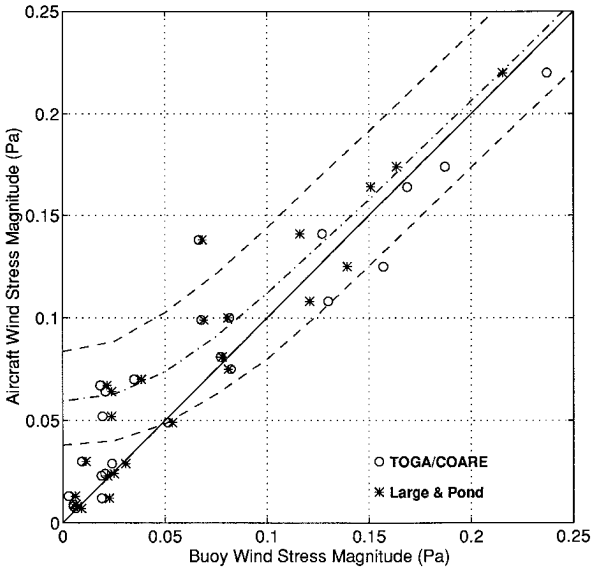

FIG. 5. Comparison of aircraft and buoy wind stress magnitudes using the TOGA COARE and Large and Pond (1981) parameterizations. The solid line along the diagonal indicates a one-to-one relationship. The aircraft wind stress vector magnitudes and direction are computed from the directly measured east τ_x and north τ_y components. If we assume independent Gaussian measurement errors in τ_x and τ_y with a standard deviation of 0.05 Pa and no error in the buoy wind stress magnitude, then the expected aircraft wind stress magnitude should fall along the dash–dot line, and 50% of the aircraft wind stress magnitude data should fall within the dashed lines. The dashed lines represent the 25% and 75% of the wind stress magnitude distribution. The presence of small aircraft wind stress magnitudes less than 0.05 Pa suggests that the measurement errors can be significantly less than 0.05 Pa at low wind stresses.

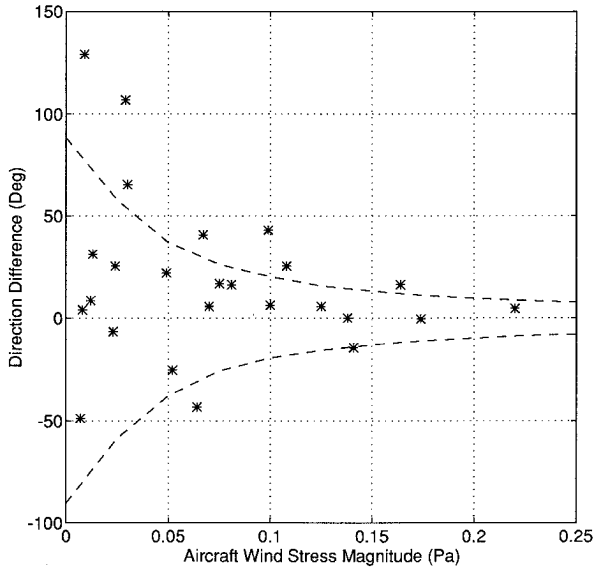

FIG. 6. The difference between the 30-m aircraft wind stress direction and the aircraft wind direction. Note at low wind stresses, the aircraft wind stress direction is more sensitive to uncertainty in the individual wind stress components. Assuming independent normal errors in τ_x and τ_y with a standard deviation of 0.05 Pa, one-half of the direction difference data, on average, should lie between the dashed lines (which represent the 25% and 75% of the direction difference distribution).

the stable platform R/P *FLIP* (Friehe et al., unpublished manuscript) show that the wind and stress vectors are aligned for steady-state conditions with wind and sea aligned.

Despite the above uncertainties, the comparison of aircraft and buoy wind stress components is good, especially at the higher winds. The correlation coefficients between aircraft and buoy wind stress components are about 0.82 for the east component and 0.98 for the north component using both parameterizations (Figs. 7 and 8; Tables 1 and 2). For the east component, the average difference and standard deviation are 0.018 ± 0.029 Pa using TOGA COARE and -0.018 ± 0.027 Pa using Large and Pond (1981). For the north component, the average difference and standard deviation are 0.003 ± 0.018 Pa using TOGA COARE and 0.003 ± 0.017 Pa using Large and Pond (1981).

For the larger stresses, the aircraft wind stress magnitudes are generally between the Large and Pond (1981) values (which are smaller) and the TOGA COARE values (which are larger). This difference is caused in part by the fact that the TOGA COARE parameterization uses the neutral 10-m drag coefficient C10N given by Smith (1988), which is larger than the Large and Pond (1981) C10N at 10-m wind speeds between about 7 and 22 m s^{-1} (Fig. 9). The buoy air–sea temperature differences are sufficiently small at the higher wind speeds during these overflights so that stability does not affect the buoy wind stress amplitude

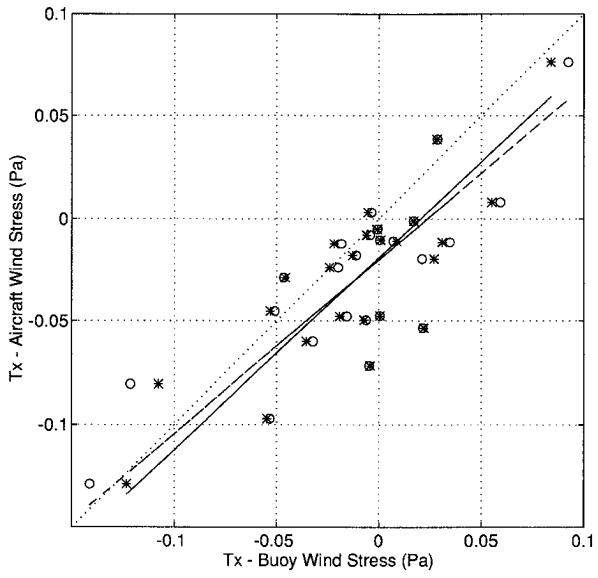

FIG. 7. The east component of aircraft and buoy wind stress using both parameterizations. The dotted line along the diagonal indicates a one-to-one relationship. The dashed line is a best fit for TOGA COARE, solid line for Large and Pond (1981). See Table 3 for regression results.

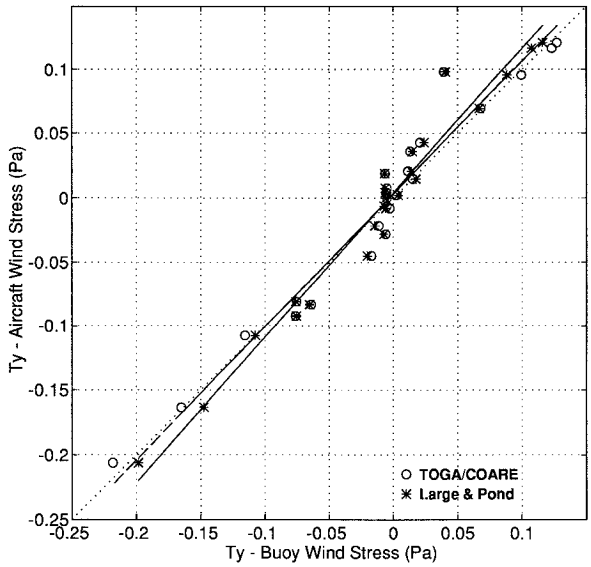

FIG. 8. The north component of aircraft and buoy wind stress using both parameterizations. The dotted line along the diagonal indicates a one-to-one relationship. The dashed line is a best fit for TOGA COARE, solid line for Large and Pond (1981). See Table 3 for regression results.

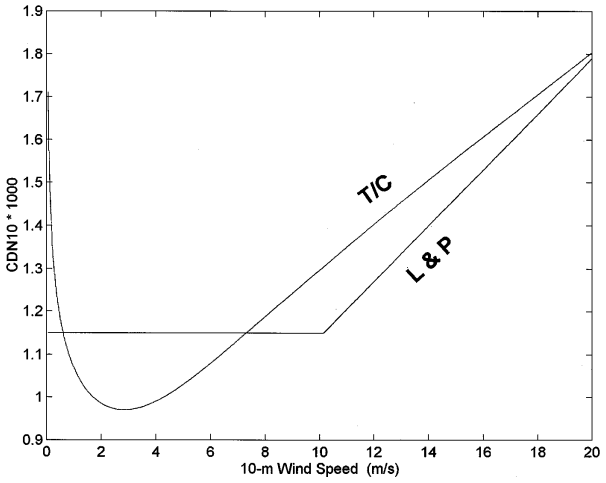

FIG. 9. The neutral 10-m drag coefficients used in the TOGA COARE and Large and Pond (1981) parameterizations plotted versus the 10-m wind speed.

appreciably. While there are insufficient data here to choose between the two parameterizations, it is reassuring that both parameterizations give similar results under these experimental conditions. Enriquez and Friehe (1996) have recently used the SMILE 30-m King Air wind and wind stress measurements to compute the drag coefficient and examine its dependence on wind speed and height and found support for the general shape of the Large and Pond (1981) parameterization.

6. Conclusions

An intercomparison between low-level aircraft measurements of wind and wind stress and buoy measurements of wind and wind stress estimated using the TOGA COARE and Large and Pond (1981) parameterizations has been made using data collected over the northern California shelf during February–March 1989. The agreement between the King Air wind speed and direction measurements obtained at 30 m and NDBC buoy wind speed and direction measurements made at 10 m is quite good. Despite the large experimental uncertainty of order ± 0.05 Pa in the aircraft wind stress estimates, the agreement between aircraft and buoy wind stress estimates at the larger wind stresses during these overflights is good using either parameterization. The 30-m aircraft wind stress direction and the 10-m buoy wind direction agree within measurement uncertainty at larger wind stresses. These results give strong support to the hypothesis that low-flying research aircraft like the King Air can be used to accurately map the surface wind stress field during even moderate wind conditions and that the dominant spatial variability found in the SMILE aircraft wind stress measurements by Enriquez and Friehe (1995) did exist at the ocean surface.

Acknowledgments. The data analyzed here were collected by the NCAR Research Aircraft Facility and the NOAA Data Buoy Center with support from the National Science Foundation and the Mineral Management Service. The TOGA COARE code (version 1.0) was supplied by D. Rogers. His assistance, plus useful discussions with J. Edson and a thoughtful review by R. Weller, are greatly appreciated. Technical information about the NDBC buoys was kindly provided by D. Gilhousen, E. Michelena, and C. Woody. An anonymous reviewer suggested the correct method to compute the nonlinear regression results presented in Table 3 and Figs. 7 and 8. This analysis effort has been supported by NSF Grants OCE 91-15713 and OCE 93-13671 and ONR N00014-92-J-1528.

TABLE 3. Regression comparison of Large and Pond (1981) and TOGA COARE wind stress components. Slope and intercept values with 95% confidence intervals (in parentheses) are computed for each component.

	Large and Pond		TOGA COARE	
	τ_x	τ_y	τ_x	τ_y
Slope	0.932 ($\pm$0.307)	1.128 ($\pm$0.095)	0.844 ($\pm$0.273)	1.036 ($\pm$0.100)
Intercept	$-$0.019 ($\pm$0.016)	0.004 ($\pm$0.009)	$-$0.020 ($\pm$0.015)	0.003 ($\pm$0.011)

REFERENCES

Alessi, C. A., S. J. Lentz, and R. C. Beardsley, 1991: Shelf Mixed Layer Experiment (SMILE) program description and coastal and moored array data report. Woods Hole Oceanographic Institution Tech. Rep. WHOI-91-39, 205 pp. [Available from Dept. of Physical Oceanography, Woods Hole Oceanography Institution, Woods Hole, MA 02543-1541.]

Beardsley, R. C., C. E. Dorman, C. A. Friehe, L. K. Rosenfeld, and C. D. Winant, 1987: Local atmospheric forcing during the Coastal Ocean Dynamics Experiment. 1. A description of the marine boundary layer and atmospheric conditions over a northern California upwelling region. *J. Geophys. Res.,* **92,** 1467–1488.

Businger, J. A., J. C. Wyngaard, Y. Izumi, and E. F. Bradley, 1971: Flux-profile relationships in the atmospheric surface layer. *J. Atmos. Sci.,* **28,** 191–199.

Dorman, C. E., A. G. Enriquez, and C. A. Friehe, 1995: Structure of the lower atmosphere over the northern California coast during winter. *Mon. Wea. Rev.,* **123,** 2384–2404.

Enriquez, A. G., 1994: Variability of the surface wind and ocean circulation over the northern California shelf. Ph.D. thesis, University of California, 213 pp. [Available from Dept. of Mechanical Engineering, University of California, Irvine, Irvine, CA 92697-3975.]

——, and C. A. Friehe, 1995: Effect of wind stress and wind stress variability on coastal upwelling. *J. Phys. Oceanogr.,* **25,** 1651–1671.

——, and ——, 1997: Bulk parameterizations of momentum, heat, and moisture fluxes over a coastal upwelling area. *J. Geophys. Res.,* in press.

Fairall, C., E. F. Bradley, D. P. Rogers, J. B. Edson, and G. S. Young, 1996: Bulk parameterization of air–sea fluxes for Tropical Ocean–Global Atmosphere Coupled Ocean Atmosphere Response Experiment (TOGA COARE). *J. Geophys. Res.,* **101,** 3747–3764.

Friehe, C. A., R. C. Beardsley, C. D. Winant, and J. P. Dean, 1984: Intercomparison of aircraft and surface buoy meteorological data during CODE-1. *J. Atmos. Oceanic Technol.,* **1,** 79–86.

——, A. G. Enriquez, and L. Tran, 1991: SMILE time series and profile plots of aircraft measurements. UCI Tech. Rep., 500 pp.

Geernaert, G. L., 1988: Measurements of the angle between the wind vector and the wind stress vector in the surface layer over the North Sea. *J. Geophys. Res.,* **93,** 8215–8220.

——, 1990: Bulk parameterizations for the wind stress and heat flux. *Surface Waves and Fluxes,* Vol. 1, G. L. Geernaert and W. Plant, Eds., Kluwer Academic, 91–172.

——, M. Hansen, and M. Courtney, 1993: Directional attributes of the ocean surface wind stress vector. *J. Geophys. Res.,* **98,** 16 571–16 582.

Gilhousen, D. B., 1987: A field evaluation of NDBC moored buoy winds. *J. Atmos. Oceanic Technol.,* **4,** 94–104.

Large, W. G., and S. Pond, 1981: Open ocean momentum flux measurements in moderate to strong winds. *J. Phys. Oceanogr.,* **11,** 324–336.

——, J. Morzel, and G. B. Crawford, 1995: Accounting for surface wave distortion of the marine wind profile in low-level Ocean Storms wind measurements. *J. Phys. Oceanogr.,* **25,** 2959–2971.

Liu, W. T., K. B. Katsaros, and J. A. Businger, 1979: Bulk parameterizations of air–sea exchanges of heat and water vapor including the molecular constraints at the interface. *J. Atmos. Sci.,* **36,** 1722–1735.

Miller, E. R., and R. B. Friesen, 1985: Standard output data products from the NCAR Research Aviation Facility. NCAR RAF Bulletin 9, 9 pp. [Available from National Center for Atmospheric Research, P.O. Box 3000, Boulder, CO 80307.]

Rieder, K. F., J. A. Smith, and R. A. Weller, 1994: Observed directional characteristics of the wind, wind stress, and surface waves on the open ocean. *J. Geophys. Res.,* **99,** 22 589–22 596.

Santala, M. J., 1991: Surface-referenced current meter measurements. Ph.D. thesis, MIT/WHOI, WHOI-91-35, 284 pp. [Available from Dept. of Physical Oceanography, Woods Hole Oceanography Institution, Woods Hole, MA 02543-1541.]

Smith, S. D., 1988: Coefficients for sea surface wind stress, heat flux, and wind profiles as a function of wind stress and temperature. *J. Geophys. Res.,* **93,** 15 467–15 472.